Published in final edited form as:
J Phys Chem C Nanomater Interfaces. 2012 August 2; 116(30): 15867–15877. doi:10.1021/jp301853d.

Zirconium(IV) and Hafnium(IV) Porphyrin and Phthalocyanine Complexes as New Dyes for Solar Cell Devices

Ivana Radivojevic[†], **Giorgio Bazzan**[‡], **Benjamin P. Burton-Pye**[†], **Kemakorn Ithisuphalap**[†], **Raihan Saleh**[†], **Michael F. Durstock**[‡], **Lynn C. Francesconi**[†], and **Charles Michael Drain**[*,†,||]
Department of Chemistry and Biochemistry, Hunter College of the City University of New York, New York, New York 10065, Air Force Research Laboratory, Wright-Patterson Air Force Base, Ohio, 45433, The Rockefeller University, New York, New York 10065

Abstract

Metalloporphyrin and metallophthalocyanine dyes ligating Hf(IV) and Zr(IV) ions bind to semiconductor oxide surfaces such as TiO_2 via the protruding group IV metal ions. The use of oxophylic metal ions with large ionic radii that protrude from the macrocycle is a unique mode of attaching chromophores to oxide surfaces in the design of dye-sensitized solar cells (DSSCs). Our previous report on the structure and physical properties of ternary complexes wherein the Hf(IV) and Zr(IV) ions are ligated to both a porphyrinoid and to a defect site on a polyoxometalate (POM) represents a model for this new way of binding dyes to oxide surfaces. The Zr(IV) and Hf(IV) complexes of 5,10,15,20-tetraphenylporphyrin (TPP) with two ligated acetates, (TPP)Hf$(OAc)_2$ and (TPP)Zr$(OAc)_2$, and the corresponding metallophthalocyanine (Pc) diacetate complexes, (Pc)Hf$(OAc)_2$ and (Pc)Zr$(OAc)_2$, were evaluated as novel dyes for the fabrication of dye-sensitized solar cells. Similarly to the ternary complexes with the POM, the oxide surface replaces the acetates to affect binding. In DSSCs the Zr(IV) phthalocyanine dye performs better than the Zr(IV) porphyrin dye, and reaches an overall efficiency of ~ 1.0%. The Hf(IV) dyes are less efficient. The photophysical properties of these complexes in solution suggested energetically favorable injection of electrons into the conduction band of TiO_2 semiconductor nanoparticles, as well as a good band gap match with I_3^-/I^- pair in liquid 1-butyl-3-methyl imidazolium iodide. The combination of blue absorbing TPP with the red absorbing Pc complexes can increase the absorbance of solar light in the device; however, the overall conversion efficiency of DSSCs using TiO_2 nanoparticles treated with a mixture of both Zr(IV) complexes is comparable, but not greater than, the single (Pc)Zr. Thus, surface bound (TPP)Zr increases the absorbance in blue region of the spectra, but at the cost of diminished absorbance in the red in this DSSC architecture.

Keywords

polyoxometalate; photophysics; dye blend; titanium dioxide; panchromatic

cdrain@hunter.cuny.edu.
[†]Hunter College
[‡]Air Force Research Laboratory
[||]Rockefeller University

SUPPORTING INFORMATION AVAILABLE
Spectral characterization of the metallophthalocyanines, CV data, photophysical data, replicate DSSC data. This information is available free of charge via the Internet at http://pubs.acs.org.

INTRODUCTION

Porphyrins (Pors) and phthalocyanines (Pcs) are widely studied as photosensitizers of oxide semiconductors for use in dye-sensitized solar cells (DSSCs),[1,2] organic solar cells, and for water splitting reactions because of their large absorbance maxima, > 10^5 $M^{-1}cm^{-1}$, in the visible part of the solar spectrum. [3–12] Fine tuning the absorption properties of the Por pigments by modifications of the macrocycle is well-established in photosynthesis. Pcs are used commercially as dyes and in photonic devices such as displays, and optical recording media. The diverse photophysical and chemical properties of porphyrinoids can be tuned by metalation with almost any metal ion and/or exocyclic modification of the macrocycle to adjust excited state lifetimes, HOMO-LUMO energies, optical-cross section, and redox potentials.[13–18] Simple Por and Pc, such as those described herein, can be commercially viable dyes for solar energy applications because they can be synthesized in good yields from simple starting materials.[19] Functional supramolecular materials composed of porphyrinoids can be robust, and are useful in artificial photosynthesis in terms of light harvesting and for understanding energy and electron transfer between dyes.[20–28] Pcs are excellent candidates for solar light collection because they have strong Q bands in the red to near-IR (630–780 nm) region[29,30] where the Pors have weaker absorption bands[31] (Figure 1). The low solubility of Pc presents challenges since aggregates can have diminished effectiveness in these applications, but peripheral substitution can simultaneously improve solubility and change the HOMO-LUMO energy gap, thereby the electronic absorption spectra.[13,32] Since porphyrins have strong B band absorptions in the blue and Pc have strong Q absorptions in the red, they can be used in combination in thin film materials to broaden absorptivity compared to a single dye.[19]

The best performing Ru bipyridine complexes in DSSCs give ~11% efficiency,[33] > 80% incident photon to current efficiency (IPCE), and have a broad absorption up to ~10^4 $M^{-1}cm^{-1}$, but the cost of Ru metal and associated environmental impact limits use of these dyes in DSSCs.[34] The Ru complexes and most other sensitizer dyes are bound to the TiO_2 semiconductor by carboxylic acid group(s) either appended directly to the chromophore or through an intervening tether.[35] Other modes of attachment include phosphonates and sulfonates, which tend to bind stronger to the oxide surface, but so far these DSSCs are less efficient.[36–38] Lin and corkers describe several push-pull porphyrin systems attached to the oxide surface through carboxylic groups and a conjugated tether that are over 10% efficient.[39–42] The efficiency with another specially designed “push-pull” Por is ca. 12% efficient reported by Grätzel and coworkers.[1,7,43] Using push-pull(Pc)Zn with carboxylic acid groups for binding and *t*-butyl groups to increase solubility and tune directionality of electron flow results in DSSC with η=3.52% and an IPCE of 47% at the λ_{max}. Though Pc systems with up to 75% IPCE can be made, the efficiencies are low.[12,44,45] Beside the type of binding and the composition of the anchoring group, the orientation and packing of the dyes play important role in injecting electrons from the LUMO orbital of the dye to the conduction band of oxide semiconductor.[46–48] Galoppini and coworkers studied the influence of orientation and position of carboxylic binding on electronic and chemical properties of different free base and Zn(II) porphyrins.[48,49] Other orthogonal vs. planar dye orientations were studied.[50,51] Though free base and Zn(II) tetracarboxyphenylporphyrin have almost the same electron injection and charge recombination properties, the broader absorption of the N3 dye [cis-bis(isothiocyanato)-bis-(2,2′-bipyridyl-4,4′-dicarboxylato ruthenium(II)] results in better DSSCs.[52–54] Panchromatic cosensitization is a viable approach that combines different dyes to broaden the absorption spectra; however, to date the efficiency is lower or between the two individual dyes since the dyes are competing for the same space on the semiconductor. [44,55–57]

Since polyoxometalates (POMs) are often regarded as good models for defect sites on oxide surfaces,[58] we previously reported [59] the synthesis and characterization of ternary Zr(IV) and Hf(IV) complexes of tetraphenylporphyrin (TPP) and tetrapyridylporphyrin bound to a monovacant Keggin POM, $PW_{11}O_{39}^{7-}$. The POM studies suggested that one way to append porphyrinoids onto TiO_2 surfaces is to use oxophylic, Hf and Zr ions that protrude from one face of the macrocycle. Upon displacement of the auxiliary acetate ligands, the metal ions of $Hf(Por)^{2+}$ and $Zr(Por)^{2+}$ are bound to oxide surfaces, e.g. at defects, via the four open metal ion coordination sites.[59] Since the metal ion is simultaneously bound to the oxide surface and to the porphyrin and the chromophore orbitals are strongly coupled with the metal ion orbitals,[60] the overall hypothesis is that this mode of binding facilitates charge injection via both the metal ion and the proximity of the dye to the surface. The Pc-Zr(IV)-POM and Pc-Hf(IV)-POM ternary complexes can be synthesized similarly to the corresponding Por-M-POM ternary compounds[59] which provide a basis for the proposed bonding of the (Pc)Hf(IV) and (Pc)Zr(IV) dyes to the oxide surfaces such as anatase TiO_2 [61,62] (Figure 2).

The overarching goal of the present work is to examine the functionality of Hf(IV) and Zr(IV)Pc and Por dyes in DSSCs. Herein we report the photophysical properties of the metalloporphyrins compared to the metallophthalocyanines, $(Pc)Hf(OAc)_2$ and $(Pc)Zr(OAc)_2$ to $(TPP)Zr(OAc)_2$ and $(TPP)Hf(OAc)_2$, and the performance of DSSC using this new mode of binding sensitizers to porous nanocrystaline semiconductor oxide surfaces (Figure 2). The performance of photovoltaic solar cells using a TiO_2 nanoparticle semiconductor layer sensitized with one of the four dyes allows an assessment of the feasibility of using a combination of Por and Pc to capture the blue and red region of solar spectra, respectively. We find that the (TPP)Hf and (Pc)Hf complexes are not as efficient in these DSSC devices as the (TPP)Zr and (Pc)Zr complexes, so focus on the latter herein (see ESI).

EXPERIMENTAL SECTION

Materials—Toluene, dichloromethane, pyridine, acetonitrile, ITO coated glass slides, titanium(IV) dioxide nanopowder, (TiO_2, 99.7%, anatase) tetra(*n*-butyl) ammonium hexafluorophosphate (Bu_4NPF_6), ferrocene, and $AgNO_3$ were purchased from Sigma Aldrich and used as received. The Hf(IV) and Zr(IV) porphyrinates were synthesized as previously reported.[59,63]

Instrumentation—UV-visible spectra were taken in 1 cm quartz or glass cuvettes using a Cary Bio-3 spectrophotometer. Solution phase fluorescence spectra were taken in right angle mode using a Horiba Jobin Yvon Fluorog-3 instrument, as were phosphorescence data using a FL-1040 attachment. Fluorescence lifetimes were measured using a Fluorog-3 time correlated single photon counting (TCSPC) instrument using NanoLed lasers at 405 nm or 670 nm for excitation of metalloporphyrin and metallophthalocyanine compounds, respectively. Fitting software was provided with the instrument. A home-built ozone cleaner was used to clean the ITO substrates. Cyclic voltammetry measurements were performed with a BASi Voltammetric Analyzer System controlled by BASi CV-50W software in a conventional three-electrode electrochemical cell, using a platinum wire as the auxiliary electrode, and Ag/Ag+ as the reference electrode. Transient absorbance measurements were done at Brookhaven National Laboratories using a Helios TA Spectrometer, with a 1 kHz amplified Ti:Sapphire based laser. Photovoltaic measurements were made at Wright-Patterson Air Force Base with a class-A 450W Oriel Solar Simulator (Model 91195-A) equipped with an AM1.5 global filter. The power of the simulated light was calibrated to 100 mW/cm^2 using a Newport Radiometer.

Synthesis of the Pc dyes

Hafnium (IV) phthalocyaninato diacetate, (Pc)Hf(OAc)$_2$—(Pc)Hf(Cl)$_2$ was prepared according to the literature.[64–66] 0.4 mL of trichlorobenzene in a 18×150 mm test tube containing a stir bar was heated in a sand bath to > 100 °C, whereupon 0.8 mg (6.3 mmol) dicyanobenzene and 0.218 mL (1.5 mmol) 2-methylnaphthalene were added and heated > 200 °C. When the reaction mixture clarified, 500 mg (1.5 mmol) of $HfCl_4$ was added to the solution and the reaction mixture turned dark yellow. After heating under reflux for 1 h the solution was a dark brownish green color. When cooled to 50 °C, the solution was filtered and rinsed with methanol to yield a dark blue solid. 200 mg of (Pc)Hf(Cl)$_2$ (763.94 g/mol) was dissolved in a minimum amount of DMSO in a 18×150 mm test tube with a stir bar at room temperature, loaded onto silica gel in a glass frit filter, then placed on a filtering flask under vacuum. The sample was washed with methanol to remove the DMSO. (Pc)Hf(OAc)$_2$, was eluted with 3:1:1 mixture of CH_2Cl_2:methanol:acetic acid. This procedure exchanges the chlorides for the acetates concomitant with purification, and is similar to the preparation of corresponding metalloporphyrin acetate complexes.[59,63] The solvent was removed by rotary evaporation, the dried solid re-dissolved in CH_2Cl_2, filtered, and precipitated with hexane to yield 166 mg of a dark blue solid (83%). ($C_{36}H_{16}N_8$)Hf($C_2H_3O_2$)$_2$: 1H NMR (500 MHz, $CDCl_3$) δ ppm: 9.48 (br s, 8H, H^{α}), 8.23 (br s, 8H, H^{β}), 0.41 (br s, 6H, OAc). UV-Vis. in CH_2Cl_2 λ_{max} nm (log ε): 334 (6.04), 614 (5.73), 652 (5.67), 684 (6.49). MALDI-MS m/z=807.2 calcd., found 807.17

Zirconium(IV) phthalocyaninato diacetate (Pc)Zr(OAc)$_2$—This complex is prepared similarly to the hafnium complex except using (Pc)Zr(Cl)$_2$ (676.67 g/mol) as the starting reactant.[64–66] This compound was more difficult to isolate as a solid product after metal ion insertion. (Pc)Zr(Cl)$_2$ was prepared by adding 2 mL trichlorobenzene in a 18×150 mm test tube containing a stir bar, heating in a sand bath to > 100°C, whereupon 0.517 mg (4 mmol) dicyanobenzene and 0.165 mL (1.1 mmol) 2-methylnaphthalene were added and heated > 200°C. When the reaction mixture clarified, 276 mg (2 mmol) of $ZrCl_4$ was added to the solution and the reaction mixture turned dark yellow. After heating under reflux for 1 h the solution was a dark brownish green color. When cooled to 50°C, the solution was filtered and rinsed with methanol. First dark green fraction was separated and contained unreacted material. The solid (Pc)$ZrCl_2$ product was isolated on filter paper and was loaded onto 30 g of silica and eluted with 3:1:1 mixture (CH_2Cl_2:methanol:acetic acid) to exchange the auxiliary chloride counter ions. After removing the solvent, the solid was re-dissolved in CH_2Cl_2, filtered, and precipitated with hexane to yield 230 mg of a green solid (~84%). ($C_{36}H_{16}N_8$)Zr($C_2H_3O_2$)$_2$: 1H NMR (500 MHz, $CDCl_3$) δ ppm: 9.43 (br s, 8H, H^{α}), 8.20 (br s, 8H, H^{β}), 0.42 (br s, 6H, OAc). UV-Vis. CH_2Cl_2 λ_{max} nm (log ε): 336 (6.01), 616 (5.64), 652 (5.58), 685 (6.35). MALDI-MS m/z=721.5. calcd., found 720.17 (see ESI).

Binding of (Pc)Hf(OAc)$_2$ and (Pc)Zr(OAc)$_2$ on TiO_2—0.8 mg of (Pc)Hf(OAc)$_2$ or (Pc)Zr(OAc)$_2$ was dissolved in 2 mL of distilled toluene and ca. 30 mg TiO_2 nanopowder, (99.7% anatase with average size 5 nm) was added to the solution. After sonicating for 5 min, the slurry was stirred overnight. The supernatant remained colored indicating that the solid was saturated with the dye. The slurry was then centrifuged for 5 min to separate the coated particles, which are blue colored due to the bound Hf(Pc)$^{2+}$ or Zr(Pc)$^{2+}$ on TiO_2. The solution was decanted, the coated particles were rinsed with toluene 2–3 times to remove unbound materials, and left to dry in air. Similar treatment binds the TiO_2 particles with the group (IV) metal ion complexes of TPP derivatives.[59] In control experiments, most of the dye remains in solution when (Pc)Zn(II) or free base Pc are used, or the free base TPP or (TPP)Zn(II).[59]

Electrochemical Measurements—For cyclic voltammetry, a three electrode, one compartment electrochemical cell was used. The reference electrode was Ag/Ag+ with (0.01 M $AgNO_3$/0.1 M Bu_4NPF_6/CH_3CN); auxiliary electrode was Pt and working electrode was ITO coated glass slide (0.5 cm×2.5 cm); supporting electrolyte used was 0.1 M Bu_4NPF_6/CH_2Cl_2. All redox potentials were referenced against ferrocene (Fc+/Fc) internal standard. The electrolyte solution was de-gassed with nitrogen prior to measurements. Peaks potentials were measured at different scan rates. The ITO slides were cleaned by a piranha solution (3:1 NH_4OH/H_2O_2 for 30 min) followed by rinsing with copious amounts of water just prior to using. The concentration of the solution in CH_2Cl_2 in all experiments was ~1 mM.

Transient Absorbance Measurements—Femtosecond and nanosecond transient absorbance measurements were performed in the Brookhaven National Laboratory at the Center for Functional Nanomaterials, Ultrafast Optical Spectroscopy Facility using a 1 kHz Ti:Sapphire based laser. Resonant excitation in the ultraviolet and visible was achieved using a tunable optical parametric amplifier and samples were probed using a laser generated supercontinuum. For femtosecond measurements, the supercontinuum was derived from a mechanically delayed portion of the laser fundamental focused into a sapphire plate system with 100 fs time resolution. For nanosecond measurements, an electronically synchronized fiber source was used, with approximately 500 ps time resolution. Femtosecond time-resolved photoluminescence spectra were measured using the upconversion technique. Excitation pulses from the same ultrafast laser system were used to resonantly excite the samples. Spontaneous emission was collected with a set of lenses and focused in a nonlinear crystal, where it is mixed with a 100 fs gate pulse. The upconverted photons generated via the sum frequency interaction are directly detected as a function of time delay between the excitation and gate pulse. All measurements were performed at room temperature, with or without argon flow. The optical density used in the pump-probe experiments was < 0.4 in a 2 mm quartz cuvette at 540 nm for porphyrin compounds and < 0.4 at 685 nm for phthalocyanine compounds. The steady state absorption spectra were taken after the measurements to check for sample photobleaching and degradation. Degradation was observed for porphyrin samples which led to more frequent changing of the samples and the use of an argon flow throughout some of the experiments.

Device Fabrication—Well-established procedures for the fabrication of Grätzel-type dye-sensitized solar cells were used in our experiments.[67] Briefly, the devices were assembled in a typical sandwich-type format, using fluorine-doped SnO_2 (FTO) conductive glass substrate (sheet resistance 14 Ω/square, Hartford Glass Co. USA) pretreated with a 40 mM aqueous solution of $TiCl_4$ at 70 °C for 30 min. Mesoporous titania film were prepared by doctor-blading a suspension of 20 nm diameter nanoparticles (Ti-Nanoxide T20 from Solaronix S.A., Lausanne, Switzerland) that resulted in an uniform film with a thickness of 8–9 μm after sintering at 500 °C for 30 min. A light scattering-layer of TiO_2 400 nm nanoparticles was deposited on the top of the film for a total electrode thickness of 13.5–14.5 μm. The cell was completed using a thermally platinized FTO counter electrode and a 25 μm thick Surlyn spacer (Solaronix-SX1170 hot melt film). Dyes, (Pc)Zr/Hf$(OAc)_2$, (TPP)Zr/Hf$(OAc)_2$, and mixture of (Pc)Zr/Hf$(OAc)_2$/(TPP)Zr/Hf$(OAc)_2$ were adsorbed onto TiO_2 layer. The concentration of the dye solution for binding to the TiO_2 film was either 0.3 mM or 0.1 mM in CH_2Cl_2(see discussion). For experiments with mixture of dyes, solutions of the same concentration of the individual dyes were mixed prior to emersion of the TiO_2 electrode in solution. Electrode was immersed overnight in dye solution. Afterwards, the TiO_2 layer was thoroughly rinsed with pure solvent to remove excess dye and then dried. The electrolyte solution was comprised of 1-butyl-3-methyl imidazolium iodide (0.6 M), I_2 (0.03 M),

guanidinium thiocyanate (0.10 M), and 4-tertbutylpyridine (0.5 M) in a mixture of acetonitrile and valeronitrile (85:15, v:v).

Photocurrent-Voltage and IPCE Measurements—The incident photon-to-current efficiency (IPCE) measurements were performed on the same sandwich type cells used for the I–V measurements. The IPCE of the cells were measured in DC mode using a SRS SR570 current sensitive preamplifier connected to a Keithley 2000 digital multimeter. The probe beam consisted of light from a 50 Watt tungsten-halogen lamp passed through an Acton Spectrapro-275 monochromator with order sorting filters in the range of 375–850 nm. The IPCE was determined ratiometrically by comparing the spectrum of the device with that of a calibrated Hamamatsu photodiode with an area of 1 cm^2. N719 was used as a standard (see ESI).

RESULTS AND DISCUSSION

The starting $(Pc)Hf(Cl)_2$ and $(Pc)Zr(Cl)_2$ were synthesized by building the phthalocyanine ring around a central metal ion,[65] followed by efficient exchange of the chlorides for acetates by elution over a silica column.[63] Though the literature reports that $(Pc)Zr(Cl)_2$ can easily be isolated as solid product,[65] we found that careful washing of the reaction mixture yields two soluble components that were separated by color. The first dark green/brown fraction contained the unreacted material followed by a 2nd green/blue fraction containing the dichloride salt. In the case when solid $(Pc)Zr(Cl)_2$ was not readily available, the 2nd fraction was used to prepare the bright green $(Pc)Zr(OAc)_2$.

Energy Level Calculations

The energy level diagram for the components of our solar device is shown in Figure 3, and the values of excitation energy, ground state and excited state oxidation potentials of the dyes are summarized in Table 1. The oxidation potential of the excited state, $E_{ox}^*(S^*/S^+)$ in V can be calculated from the ground state oxidation potential and the excitation energy according to equation 1.[68,69]

$$E_{ox}^*(S^*/S^+)=E_{1/2}(S/S^+)-E_{0-0}/F \quad \text{(eq. 1)}$$

where $E_{0\text{-}0}$ is the excitation energy (eV) and F is the Faraday constant = 96485 Q* mol^{-1}. The oxidation potential of the ground state is acquired from cyclic voltammetry data, while excitation energy $E_{0\text{-}0}$ is estimated from the intersection of the normalized emission and absorption spectra of the dye (ESI). For all four metalated dyes, electron injection is energetically favorable relative to the conduction band of TiO_2 and also favorable relative to I_3^-/I^- electrolyte that serves to regenerate the dye by electron transfer from I^-. The mismatch between the dye oxidation potential and electrolyte reduction potential has a significant deleterious impact by lowering the open circuit voltage (V_{oc}) in dye-sensitized solar cells.[11] The phthalocyanine dyes have an advantage since the ground state oxidation potential lies less positive vs NHE making the mismatch with the I_3^-/I^- redox pair smaller, ~ 370 mV. The regeneration of the dye by the redox pair is a two electron process that has a large driving force (600 mV) for most of the Ru dyes, and it is approximately the same for porphyrin dyes.[11]

Photophysical Properties

The UV-visible reflectance absorption spectra of TiO_2 nanoparticles treated with $(Pc)Hf(OAc)_2$ or $(Pc)Zr(OAc)_2$(Figure 4) shows that the group (IV) metal ion complexes bind to the oxide surface to a greater extent than theadsorption of the free base Pc and the

(Pc)Zn. Rinsing the nanoparticles with solvent removes almost all the free base or the (Pc)Zn(II) dyes (ESI). Since most organic dyes cannot cover the entire solar energy spectrum well, using several chromophores that absorb at different wavelengths can increase the efficiency of devices by absorbing a broader spectrum of light.[4] Thus, we also examined combining these red absorbing (500–750nm) metallophthalocyanines with the corresponding blue absorbing (370–500 nm) metalloporphyrins previously reported.[59,63] UV-visible spectra reveal that mixing the (Pc)$Zr(OAc)_2$ and (Por)$Zr(OAc)_2$ dyes in solution before adsorbing them to the TiO_2 yields a film with both dyes bound to the nanoparticles (Figure 4).

Transient Absorbance

Porphyrins: (TPP)$Hf(OAc)_2$ and (TPP)$Zr(OAc)_2$—$S_0 \rightarrow S_2$ transitions from the ground state are assigned to the Soret or B band, and transitions from $S_0 \rightarrow S_1$ to Q bands.[70] The emission spectra for these complexes have a Stokes shift of ~10 nm indicating that there are small differences between ground and excited state due to vibrational/conformational differences, which is typical of many porphyrins.[71] The electronic spectra of the Zr(IV) and Hf(IV) complexes of TPP are quite similar (Table 2). Holten and coworkers have examined the photophysical properties of the $(TPP)_2Zr$ and $(TPP)_2Hf$ sandwich compounds,[72] but the excited state dynamics of (TPP)$Hf(OAc)_2$ and (TPP)$Zr(OAc)_2$ are heretofore not reported (Table 3). Transient absorbance (TA) spectra in toluene were acquired by pumping at 420 nm and probing at 540 nm. The excitation and subsequent relaxation of the B band leads predominately to the population of the lowest singlet excited state (S_1), but higher excited states can be filled as well. For porphyrins in general, excited state absorption of S_2, S_1 and T_1 is characterized by strong bleaching in the ground state corresponding to the B band, and weaker bleaching from Q bands. The relaxation of the S_2 to S_1 state can be observed as a rise in the magnitude of the S_1 bleach in the first few ps. The TA data (Table 3) indicates that the S_2 to S_1 vibrational relaxation process occurs in ~1.5 ps for (TPP)$Hf(OAc)_2$, and ~1.1 ps for (TPP)$Zr(OAc)_2$ (Figure 5A and ESI). After excitation of the S_2 state in fluorescence up-conversion measurements of (TPP)$Hf(OAc)_2$ a rise time comparable to the vibrational relaxation to S_1 was observed. For (TPP)$Hf(OAc)_2$ the ~56 ps lifetime of the decay of S_1 observed in PL up-conversion measurements agrees well with the value of ~55 ps extracted from examining the singlet dynamics in transient absorption experiments (Figure ESI S14). The fluorescence lifetime of (TPP)$Zr(OAc)_2$ was measured using time correlated single photon counting (TCSPC) by exciting at 405 nm and measuring at 633 nm in the strongest emission band. The lifetime in air, τ_{fl} ~0.602 ns, was found to be similar to the lifetime in argon, τ_{fl} ~0.572 ns. This lifetime corresponds to decay of S_1 state at the stimulated emission peak in the TA data, τ ~587 ps (Figure 5B).

For the long-lived state of (TPP)$Hf(OAc)_2$, different time constants were observed for experiments done when argon was bubbled through the solution (τ_1=4.8 μs and τ_2=25 μs) versus in air (τ =672 ns), (ESI Figure S14). For (TPP)$Zr(OAc)_2$ the two lifetimes under argon were τ_1 ~3.1 μs and τ_2 ~ 8.2 μs (Figure 5C). Triplet excited state porphyrinoids are reactive with ground state triplet oxygen,[73] thus the shorter lifetime in air confirms our assignment of the triplet state. The (TPP)Zn S_1 state decays in 2 ns predominantly by intersystem crossing to T_1 (12 ns for free base TPP).[71,74] Heavier atoms such as Hf and Zr further enhance inter system crossing (ISC), so the T_1 state becomes more efficiently populated due to the greater spin orbit coupling and ISC dynamics for (TPP)$Hf(OAc)_2$ are much faster compared to (TPP)$Zr(OAc)_2$.[72,75,76] Energy level diagrams for (TPP)$Hf(OAc)_2$, (TPP)$Zr(OAc)_2$, and the singlet dynamics representation are shown in the ESI. Though some palladium and platinum porphyrins are known to phosphoresce at RT in solution,[75] we only detected a phosphorescence band at 715 nm for (TPP)$Hf(OAc)_2$ by mixing a small amount

of solution into deaerated heavy mineral oil (Figure S17). This is in agreement with Knor et al.[75] who reported a phosphorescence quantum yield to be 8×10^{-5}.

Phthalocyanines: (Pc)Hf(OAc)$_2$ and (Pc)Zr(OAc)$_2$—The timescales attributed to singlet excited states are slower for metallophthalocyanine acetate complexes, and similar heavy atom effects were observed. The samples were pumped in the 685 nm Q band and probed at 695 nm; see ESI for energy level diagrams of singlet state dynamics. The TA experiments on (Pc)Zr(OAc)$_2$ indicate a S_1 time constant of ~1.0 ns, and for (Pc)Hf(OAc)$_2$ S_1 is ~139 ps (Figure 6A and S15A). For the Zr complex, time correlated single photon counting data exhibits a biexponential curve consisting of ~60% of a species that decays to ground state with fluorescence lifetime of 1.1 ns, and 40% at τ = 2–3 ns. Because of efficient entry into the triplet manifold, Pc also react with triplet oxygen.[77,78] In air, transient absorbance data of (Pc)Hf(OAc)$_2$ and (Pc)Zr(OAc)$_2$ in toluene show similar triplet lifetimes (~228 ns and ~223 ns). Under Ar, the triplet (Pc)Hf(OAc)$_2$ decays with a lifetime of τ ~2 μs, and (Pc)Zr(OAc)$_2$ τ ~8 μs (Figure 6B and S15B).

Quantum Yields—The fluorescence quantum yields (Φ_F) were calculated using comparative method of Williams et al. using a standard sample with known Φ_F value as reference compound (e.g. TPP, (TPP)Zn or (Pc)Zn).[79] The samples, in toluene for the metalloporphyrins and DMSO for metallophthalocyanines, were excited in Q bands where absorbance was the same for the reference and analyzed compounds. As expected for enhanced crossing to the triplet manifold, Φ_F are significantly lower for both the metallo dyes. Fluorescence lifetimes and quantum yields are summarized in Table 2. Previous reports on the fluorescence of (Pc)Hf(carboxylate)$_2$ λ_{max} = 697 nm, λ_F = 0.009, and a range of τ= 1 ns to 9.03 ns.[66] Note that charge injection from the triplet state in some dye systems, e.g. (Pc)Ru, can be efficient in DSSC.[71,74,77,80,81]

Photovoltaic Properties

The current-voltage (I–V) characteristics of devices prepared by using 0.1 mM (TPP)M(OAc)$_2$, (Pc)M(OAc)$_2$, and a 1:1 mixture of the two dyes were determined under irradiation with simulated solar light of 100 mW/cm^2 intensity (Figure 7). Table 4 shows the performance characteristics of photovoltaic cells sensitized with Zr dyes, which are significantly better than cells made with the corresponding Hf complexes. The best performing devices were obtained using (Pc)Zr dye producing an efficiency (η) of 1.05%, and devices prepared with (TPP)Zr displayed efficiencies of η=0.47%. Interestingly, light soaking of the devices prepared with our dyes resulted in an increase in the devices performance, and indicates stability to photobleaching. One hour of light soaking improves the cell efficiency by ~30% and performance increase as high as 50% are reached with 3 h of light soaking after which no further changes are observed. This phenomenon can be explained by reorganization of the dye molecules on the TiO_2 surface.[82–84] The increased efficiency is largely due to increased J_{sc}, indicating better charge injection into the semiconductor.

Devices prepared with (Pc)Zr perform better than those using (TPP)Zr, likely because the latter absorb in a region of the solar spectrum with greater solar irradiance (Figure 1), and may cover more of the TiO_2 surface because of the absence of the orthogonal phenyl groups that inhibit TPP binding via the coordinated metal ion. Moreover, the ~370 mV mismatch of the HOMO orbitals of (Pc)Zr with the I_3^-/I^- redox pair is smaller, thus reducing energetic losses compared to the ~600 mV mismatch for (TPP)Zr.

In an attempt to load more dye molecules on the TiO_2 surface, devices were prepared using a greater concentration of the sensitizer solution (0.3 mM), but these performed worse than

those prepared using 0.1 mM solution of the dye (ESI). The decreased efficiency may arise from a greater aggregation of the dye molecules resulting in increased non-productive decay of the excited states and lower V_{oc} values.[85] The tendency of Por and Pc to aggregate on TiO_2 surface can be suppressed by addition of coadsorbers,[86] as shown by Wamser et al. whose work shows efficiencies of about 3% using 0.1 mM solution of tetracarboxyphenylporphyrin in combination with 2 mM deoxycholic acid.[87]

Though devices prepared using Hf dyes do not perform as well (see ESI Table S2 and Figure S18), similar increases in efficiencies are obtained on 5 day old devices after 1 h light soaking using the (Pc)Hf dye (η=0.59%), while cells prepared with (TPP)Hf reached η=0.25%. Since Hf complexes are less stable than Zr complexes towards demetalation,[59] we suspect that the Hf bound chromophores demetalate in the DSSC either due to the electrolyte competing for the metal center and/or upon illumination. The shorter S_1 lifetime for the (Pc)Hf and increased intersystem crossing to the triplet manifold may also decrease the yield of charge injection.

(Pc)Zn sensitized DSSC devices with a 7–8 μm electrode and a 5 μm scattering layer recently were reported to have efficiencies up to 4.6%.[88] The presumed orientation of both of these systems, and others with anchoring groups appended to the macrocycles, is with the plane of the chromophore at a large angle relative to the surface of the TiO_2. This allows more dyes to pack onto the surface and increases the active layer absorptivity relative to attaching the dyes via the central metal ion where the macrocycle is nearly coplanar with the surface (Figure 2). Other oxophylic metal ions with smaller ionic radii reside within the plane of the macrocycles, e.g. Al(III), Sn(IV), Si(IV), precluding multivalent binding to the semiconductor oxide surface as found for the Hf(IV) and Zr(IV) complexes, but can bind via an oxo-bridge.[89] Since Jsc is directly related to light harvesting and electron injection efficiency, the direct consequence of a lower dye density on the TiO_2 surface, as indicated in table 4, is a lower photocurrent. Another consequence of the lower dye density on the TiO_2 surface is an increase of interfacial recombination that produces a lower photovoltage.[54] Most reported DSSC with simple, commercially viable metallo Pc have efficiencies of η < 0.1, e.g. for ZnO devices.[90] Even though the IPCE can be near 90% in the ~420 nm Soret band for a Zn(II) porphyrin,[91] η< 0.5 because this narrow electronic band absorbs a small region of the solar spectrum.

Adsorbing the complementary dyes on the TiO_2 surface from a 1:1 mixture of 0.1 mM solutions results in devices with efficiencies near those based on (Pc)Zr alone, where η ~1.0% (Table 4). The reflectance spectra indicates that more of the (Pc)Zr binds to the TiO_2 than the (TPP)Zr, which may indicate that the porphyrin molecules bind less strongly and to fewer sites on the oxide surface because of the steric interactions between the phenyl groups and the surface.[59] The Por complexes compete with (Pc)Zr for the binding sites available on the TiO_2 surface. Our interpretation of this result is that the additional blue light absorption by the (TPP)Zr is not sufficient to make up for the loss in red light absorption by the (Pc)Zr. Similar results were observed for devices made from a mixture of (Pc)Hf and (TPP)Hf dyes (Figure S18 and Table S2). The IPCE curves show maximum value of (TPP)Zr of 15% at the Soret band and 35% for (Pc)Zr at the Q band, which is consistent with the values of η for these devices. Since the photocurrent action spectra of the mixed-dye devices resembles the corresponding absorption spectra of the solutions (compare Figure 4C to 7C), both dyes are involved in the photon to current conversion and significant quenching of the (TPP)Zr in the device by electron or energy transfer to the phthalocyanine is not indicated. These devices tend to retain the same efficiency after 15 days from assembling, indicating good chemical, photo, and thermal stability of the tested dyes.

CONCLUSIONS

New metalloporphyrins and metallophthalocyanines were synthesized to investigate a new mode of binding chromophores to oxide surfaces in DSSC through group IV metal ions. The oxophylic Hf(IV) and Zr(IV) ions protrudes sufficiently from the chromophores to concomitantly bind to oxide surfaces. We hypothesized that this unique way of attaching dyes to the surface facilitates electron injection to the semiconductor because of the coupling of the dye orbitals with the Hf(IV) and Zr(IV) orbitals,[92,93] and simultaneously to the 3d orbitals of the conduction band of TiO_2.[94] Electrochemical and photophysical studies of the dye solutions show the electrochemical potential and the lifetimes of both the singlet and triplet states are adequate for electron injection into the semiconductor. The Zr complexes of both Pc and Por gave overall efficiencies of up to 1.05% and 0.47%, respectively, while the Hf complexes performed about half as well. Cosensitization of nanocrystline TiO_2 nanoparticles with both (TPP)Zr and (Pc)Zr dyes showed that random mixing of dyes does not improve performance of the solar cell. The increased absorption of blue light is offset by the decreased absorption of red light where there are more photons to be captured. Since the λ_{max} of Pc can be tuned from about 650 nm to 830 nm and the complexes can be blended into effective solar cell devices, one strategy to improve this dye system may be to use a series of (Pc)Zr(IV).[19,77] Similarly, chlorins, isobacteriochlorins, and bacteriochlorins have red-shifted Soret bands and stronger Q bands than TPP,[23,95] or multichomophore arrays wherein the attaching moiety is the Zr complex.[13,15,19,21,96] Though designed porphyrins and phthalocyanines that are made in low synthetic yields can have better performance, we focus on commercial viable dye systems that can be made in good yields using green chemistry and click-type reactions to append exocyclic motifs.[97,98] Addition of cooadsorbants to the system, which are reported to suppress aggregation of porphyrinoid dyes and to reduce back electron transfer,[87,99] may improve the performance as well.

Supplementary Material

Refer to Web version on PubMed Central for supplementary material.

Acknowledgments

This work was supported by the National Science Foundation (NSF): CHE-0847997 to C.M.D. and 0750118 to L.C.F. and to Heavy Element Chemistry Office of science, Department of Energy DE-FG02-09ER16097 to L.C.F. Hunter College science infrastructure is supported by the NSF, the National Institutes of Health (including RCMI program, RR03037 and MD007599), and CUNY. Research was carried out in part at the Center for Functional Nanomaterials, Brookhaven National Laboratory, which is supported by the U.S. Department of Energy, Office of Basic Energy Sciences, under Contract No. DE-AC02-98CH10886; and in part at the Air Force Research Laboratory's (AFRL) supported by the Materials and Manufacturing Directorate and the Air Force Office of Scientific Research (AFOSR). We would like to thank Dr. Charles T. Black and Dr. Matthew Sfeir at the CFN for their assistance in using the facility. We thank Dr. Alexander Falber for some of the characterization of the $(Pc)Zr(OAC)_2$.

References

1. Yella A, Lee HW, Tsao HN, Yi C, Chandiran AK, Nazeeruddin MK, Diau EWG, Yeh CY, Zakeeruddin SM, Gratzel M. Science. 2011; 334:629–634. [PubMed: 22053043]
2. Ning Z, Fu Y, Tian H. Energy Environ Sci. 2010; 3:1170–1181.
3. Walker B, Kim C, Nguyen TQ. Chem Mater. 2011; 23:470–482.
4. Varotto A, Nam CY, Radivojevic I, Tome JPC, Cavaleiro JAS, Black CT, Drain CM. J Am Chem Soc. 2010; 132:2552–2554. [PubMed: 20136126]
5. Darwent JR, Douglas P, Harriman A, Porter G, Richoux MC. Coord Chem Rev. 1982; 44:83–126.
6. Abe T, Tobinai S, Taira N, Chiba J, Itoh T, Nagai K. J Phys Chem C. 2011; 115:7701–7705.

7. Campbell WM, Jolley KW, Wagner P, Wagner K, Walsh PJ, Gordon KC, Schmidt-Mende L, Nazeeruddin MK, Wang Q, Gratzel M, et al. J Phys Chem C. 2007; 111:11760–11762.
8. Ooyama Y, Harima Y. Eur J Org Chem. 2009; 2009:2903–2934.
9. Imahori H, Hayashi S, Hayashi H, Oguro A, Eu S, Umeyama T, Matano Y. J Phys Chem C. 2009; 113:18406–18413.
10. Imahori H, Umeyama T, Ito S. Acc Chem Res. 2009; 42:1809–1818. [PubMed: 19408942]
11. Gratzel M. Acc Chem Res. 2009; 42:1788–1798. [PubMed: 19715294]
12. Giribabu L, Kumar CV, Reddy PY, Yum JH, Gratzel M, Nazeeruddin MK. J Chem Sci. 2009; 121:75–82.
13. Drain CM, Varotto A, Radivojevic I. Chem Rev. 2009; 109:1630–1658. [PubMed: 19253946]
14. Drain CM, Gentemann S, Roberts JA, Nelson NY, Medforth CJ, Jia S, Simpson MC, Smith KM, Fajer J, Shelnutt JA, et al. J Am Chem Soc. 1998; 120:3781–3791.
15. Drain CM, Nifiatis F, Vasenko A, Batteas JD. Angew Chem Int Ed. 1998; 37:2344–2347.
16. Dolphin, D. The Porphyrins Physical Chemistry, Part A. Vol. 3. Academic Press; New York: 1978.
17. Suslick, KS. The Porphyrin Handbook. Kadish, KM.; Smith, KM.; Guilard, R., editors. Vol. 4. Academic Press; New York: 2000.
18. Smith, KM. Porphyrins and Metaloporphyrins. Elsevier; Amsterdam: 1972.
19. Radivojevic I, Varotto A, Farley C, Drain CM. Energy Environ Sci. 2010; 3:1897–1909.
20. Drain, CM.; Chen, X. Encyclopedia of Nanoscience & Nanotechnology. Nalwa, HS., editor. Vol. 9. American Scientific Press; New York: 2004. p. 593-616.
21. Drain, CM.; Smeureanu, G.; Batteas, J.; Patel, S. Dekker Encyclopedia of Nanoscience and Nanotechnology. Schwartz, JA.; Contescu, CI.; Putyera, K., editors. Vol. 5. Marcel Dekker, Inc; New York: 2004. p. 3481-3502.
22. Milic TN, Chi N, Yablon DG, Flynn GW, Batteas JD, Drain CM. Angew Chem, Int Ed. 2002; 41:2117–2119.
23. Radivojevic I, Likhtina I, Shi X, Singh S, Drain CM. Chem Commun. 2010; 46:1643–1645.
24. Balaban TS, Linke-Schaetzel M, Bhise AD, Vanthuyne N, Roussel C, Anson CE, Buth G, Eichhofer A, Foster K, Garab G, et al. Chem Eur J. 2005; 11:2267–2275. [PubMed: 15635683]
25. Balaban TS, Berova N, Drain CM, Hauschild R, Huang X, Kalt H, Lebedkin S, Lehn J-M, Nifiatis F, Pescitelli, et al. Chem Eur J. 2007; 13:8411–8327. [PubMed: 17645286]
26. Milic T, Garno JC, Batteas JD, Smeureanu G, Drain CM. Langmuir. 2004; 20:3974–3983. [PubMed: 15969388]
27. Gong X, Milic T, Xu C, Batteas JD, Drain CM. J Am Chem Soc. 2002; 124:14290–14291. [PubMed: 12452687]
28. Muthukumaran K, Loewe RS, Ambroise A, Tamaru Si, Li Q, Mathur G, Bocian DF, Misra V, Lindsey JS. J Org Chem. 2004; 69:1444–1452. [PubMed: 14986995]
29. Lehn JM. Science. 2002:2400–2403. [PubMed: 11923524]
30. Martinez-Diaz MV, de la Torre G, Torres T. Chem Commun. 2010; 46:7090–7108.
31. Rand BP, Genoe J, Heremans P, Poortmans J. Prog Photovolt: Res Appl. 2007; 15:659–676.
32. Rio Y, Salome Rodriguez-Morgade M, Torres T. Org Biomol Chem. 2008; 6:1877–1894. [PubMed: 18480898]
33. Chiba Y, Islam A, Watanabe Y, Komiya R, Koide N, Han L. Jpn J Appl Phys, Part 1. 2006; 45:L638–L640.
34. Gratzel M. Inorg Chem. 2005; 44:6841–6851. [PubMed: 16180840]
35. Ma R, Guo P, Yang L, Guo L, Zeng Q, Liu G, Zhang X. J Mol Structure: THEOCHEM. 2010; 942:131–136.
36. Campbell WM, Burrell AK, Officer DL, Jolley KW. Coor Chem Rev. 2004; 248:1363–1379.
37. She C, Guo J, Irle S, Morokuma K, Mohler DL, Zabri H, Odobel F, Youm KT, Liu F, Hupp JT, Lian T. J Phys Chem A. 2007; 111:6832–6842. [PubMed: 17518452]
38. Lee CY, She C, Jeong NC, Hupp JT. Chem Commun. 2010; 46:6090–6092.
39. Chang YC, Wang CL, Pan TY, Hong SH, Lan CM, Kuo HH, Lo CF, Hsu HY, Lin CY, Diau EWG. Chem Commun. 2011; 47:8910–8912.

40. Lan CM, Wu HP, Pan TY, Chang CW, Chao WS, Chen CT, Wang CL, Lin CY, Diau EWG. Energy Environ Sci. 2012; 5:6460–6464.
41. Wang CL, Chang YC, Lan CM, Lo CF, Diau EWG, Lin CY. Energy Environ Sci. 2011; 4:1788–1795.
42. Wang CL, Lan CM, Hong SH, Wang YF, Pan TY, Chang CW, Kuo HH, Kuo MY, Diau EWG, Lin CY. Energy Environ Sci. 2012; 5:6933–6940.
43. Wang Q, Campbell WM, Bonfantani EE, Jolley KW, Officer DL, Walsh PJ, Gordon K, Humphry-Baker R, Nazeeruddin MK, Gratzel M. J Phys Chem B. 2005; 109:15397–15409. [PubMed: 16852953]
44. Robertson N. Angew Chem Int Ed. 2008; 47:1012–1014.
45. Reddy PY, Giribabu L, Lyness C, Snaith HJ, Vijaykumar C, Chandrasekharam M, Lakshmikantam M, Yum JH, Kalyanasundaram K, Gratzel M, et al. Angew Chem Int Ed. 2007; 46:373–376.
46. de Tacconi NR, Chanmanee W, Rajeshwar K, Rochford J, Galoppini E. J Phys Chem C. 2009; 113:2996–3006.
47. Rangan S, Katalinic S, Thorpe R, Bartynski RA, Rochford J, Galoppini E. J Phys Chem C. 2010; 114:1139–1147.
48. Rochford J, Chu D, Hagfeldt A, Galoppini E. J Am Chem Soc. 2007; 129:4655–4665. [PubMed: 17385856]
49. Rochford J, Galoppini E. Langmuir. 2008; 24:5366–5374. [PubMed: 18410135]
50. Werner F, Gnichwitz JF, Marczak R, Palomares E, Peukert W, Hirsch A, Guldi DM. J Phys Chem B. 2010; 114:14671–14678. [PubMed: 20608700]
51. Clifford JN, Martınez-Ferrero E, Viterisi A, Palomares E. Chem Soc Rev. 2011; 40:1635–1646. [PubMed: 21076736]
52. Tachibana Y, Haque SA, Mercer IP, Durrant JR, Klug DR. J Phys Chem B. 2000; 104:1198–1205.
53. Clarke TM, Durrant JR. Chem Rev. 2010; 110:6736–6767. [PubMed: 20063869]
54. Gregg BA, Pichot F, Ferrere S, Fields CL. J Phys Chem B. 2001; 105:1422–1429.
55. Cid JJ, Yum JH, Jang SR, Nazeeruddin MK, Martinez-Ferrero E, Palomares E, Ko J, Gratzel M, Torres T. Angew Chem Int Ed. 2007; 46:8358–8362.
56. Clifford JN, Forneli A, Chen H, Torres T, Tan S, Palomares E. J Mater Chem. 2011; 21:1693–1696.
57. Subbaiyan NK, D'Souza F. Chem Commun. 2012; 48:3641–3643.
58. Katsoulis DE. Chem Rev. 1998; 98:359–388. [PubMed: 11851510]
59. Falber A, Burton-Pye BP, Radivojevic I, Todaro L, Saleh R, Francesconi L, Drain CM. Eur J Inorg Chem. 2009:2459–2466. [PubMed: 20543903]
60. Yao C, Yan LK, Guan W, Liu CG, Song P, Su ZM. Dalton Trans. 2010; 39:7645–7649. [PubMed: 20401364]
61. Selloni A. Nat Mater. 2008; 7:613–615. [PubMed: 18654584]
62. Olson CL, Nelson J, Islam MS. J Phys Chem B. 2006; 110:9995–10001. [PubMed: 16706458]
63. Falber A, Todaro L, Goldberg I, Favilla MV, Drain CM. Inorg Chem. 2008; 47:454–467. [PubMed: 18088113]
64. Gerasymchuk YS, Volkov SV, Chernii VY, Tomachynski LA, Radzki S. J Alloys Compd. 2004; 380:186–190.
65. Tomachynski LA, Tretyakova IN, Chernii VY, Volkov SV, Kowalska M, Legendziewicz J, Gerasymchuk YS, Radzki S. Inorg Chim Acta. 2008; 361:2569–2581.
66. Tretyakova IN, Chernii VY, Tomachynski LA, Volkov SV. Dyes Pigm. 2007; 75:67–72.
67. Ito S, Murakami TN, Comte P, Liska P, Gratzel C, Nazeeruddin MK, Gratzel M. Thin Solid Films. 2008; 516:4613–4619.
68. Junghanel, M. Novel Aqueous Electrolyte Films for Hole Conduction in Dye Sensitized Solar Cells and Development of an Electron Transport Model. der Freien Universitat Berlin; Berlin: 2007.
69. Kathiravan A, Renganathan R. J Colloid Interface. 2009; 331:401–407.
70. Gouterman, M. The Porphyrins. Dolphin, D., editor. Academic Press; New York: 1978. p. 1-153.

71. Yu HZ, Baskin JS, Zewail AH. J Phys Chem A. 2002; 106:9845–9854.
72. Bilsel O, Bucher JW, Hammerschmitt P, Rodriguez J, Holten D. Chem Phys Lett. 1991; 182:415.
73. Moor, ACE.; Ortel, B.; Hasan, T. Photodynamic Therapy. Patrice, T., editor. Vol. 2. The Royal Society of Chemistry; London: 2003. p. 19-58.
74. Baskin JS, Yu HZ, Zewail AH. J Phys Chem A. 2002; 106:9837–9844.
75. Knor G, Strasser A. Inorg Chem Commun. 2002; 5:993–995.
76. Azenha EG, Serra AC, Pineiro M, Pereira MM, Seixas de Melo J, Arnaut LG, Formosinho SJ, Rocha Gonsalves AMA. Chem Phys. 2002; 280:177–190.
77. Ogunsipe A, Chen JY, Nyokong T. New J Chem. 2004; 28:822–827.
78. Savolainen J, van der Linden D, Dijkhuizen N, Herek JL. J Photochem Photobiol A. 2008; 196:99–105.
79. Williams ATR, Winfield SA, Miller JN. Analyst. 1983; 108:1067–1071.
80. Listorti A, Lopez-Duarte I, Martinez-Diaz MV, Torres T, DosSantos T, Barnesa PRF, Durrant JR. Energy Environ Sci. 2010; 3:1573–1579.
81. Waiters VA, de Paula JC, Jackson B, Nutaitis C, Hall K, Lind J, Cardozo K, Chandran K, Raible D, Phillips CM. J Phys Chem. 1995; 99:1166–1171.
82. Armel V, Pringle JM, Forsyth M, MacFarlane DR, Officer DL, Wagner P. Chem Commun. 2010; 46:3146–3148.
83. Fischer MKR, Wenger S, Wang M, Mishra A, Zakeeruddin SM, Graätzel M, Baäuerle P. Chem Mater. 2010; 22:1836–1845.
84. Wenger S, Bouit P-A, Chen Q, Teuscher Jl, di Censo D, Humphry-Baker R, Moser J-E, Delgado JL, Martin N, Zakeeruddin M, et al. J Am Chem Soc. 2010; 132:5164–5169. [PubMed: 20307069]
85. Mozer AJ, Wagner P, Officer DL, Wallace GG, Campbell WM, Miyashita M, Sunahara K, Mori S. Chem Commun. 2008:4741–4743.
86. He J, Benko G, Korodi F, Polivka T, Lomoth R, Akermark B, Sun L, Hagfeldt A, Sundstrom V. J Am Chem Soc. 2002; 124:4922–4932. [PubMed: 11971744]
87. Cherian S, Wamser CC. J Phys Chem B. 2000; 104:3624–3629.
88. Mori S, Nagata M, Nakahata Y, Yasuta K, Goto R, Kimura M, Taya M. J Am Chem Soc. 2010; 132:4054–4055. [PubMed: 20205478]
89. Bergkampa JJ, Shermana BD, Marino-Ochoab E, Palaciosc RE, Cosad G, Moore TA, Gust D, Moore AL. J Porphyrins Phthalocyanines. 2011; 15:943–950.
90. Idowu M, Loewenstein T, Hastall A, Nyokong T, Schlettwein D. J Porphyrins Phthalocyanines. 2010; 14:142–149.
91. Subbaiyan NK, Maligaspe E, D'Souza F. ACS Appl Mater Interfaces. 2011; 3:2368–2376. [PubMed: 21623633]
92. Donohoe RJ, Duchowski JK, Bocian DF. J Am Chem Soc. 1988; 110:6119–6124. [PubMed: 22148788]
93. Liao MS, Scheiner S. J Chem Phys. 2002; 117:205–219.
94. Asahi R, Taga Y, Mannstadt W, Freeman AJ. Phys Rev B. 2000; 61:7459–7465.
95. Stromberg JR, Marton A, Kee HL, Kirmaier C, Diers JR, Muthiah C, Taniguchi M, Lindsey JS, Bocian DF, Meyer GJ, et al. J Phys Chem C. 2007; 111:15464–15478.
96. Hasselman GM, Watson DF, Stromberg JR, Bocian DF, Holten D, Lindsey JS, Meyer GJ. J Phys Chem B. 2006; 110:25430–25440. [PubMed: 17165990]
97. (a) Drain CM, Gong X. Chem Commun. 1997:2117–2118.(b) Drain, CM.; Singh, S. The Handbook of Porphyrin Science with Applications to Chemistry, Physics, Materials Science, Engineering, Biology and Medicine. Kadish, K.; Smith, KM.; Guilard, R., editors. Vol. 2. World Scientific Publisher; Singapore: 2010. p. 485-537.
98. Mayukh M, Sema CM, Roberts JM, McGrath DV. J Org Chem. 2010; 75:7893–7896.
99. Hagfeldt A, Boschloo G, Sun L, Kloo L, Pettersson H. Chem Rev. 2010; 110:6595–6663. [PubMed: 20831177]

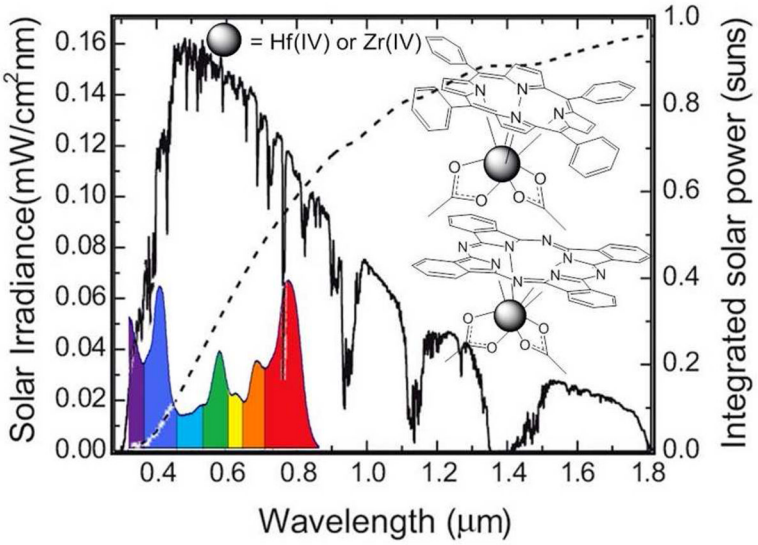

Figure 1.

A plot of the wavelength vs. solar irradiance (—), and integrated solar power (---); adapted from Poortman and coworkers, ref. 31. The strong optical absorption spectra of metallophthalocyanines (600–800 nm) and metalloporphyrins (380–450 nm) are also shown for comparison and shows that the two types of dye cover about 60% of the integrated solar power. The inset shows the Hf(IV) or Zr(IV) porphyrin on top and corresponding metallophthalocyanine on bottom.

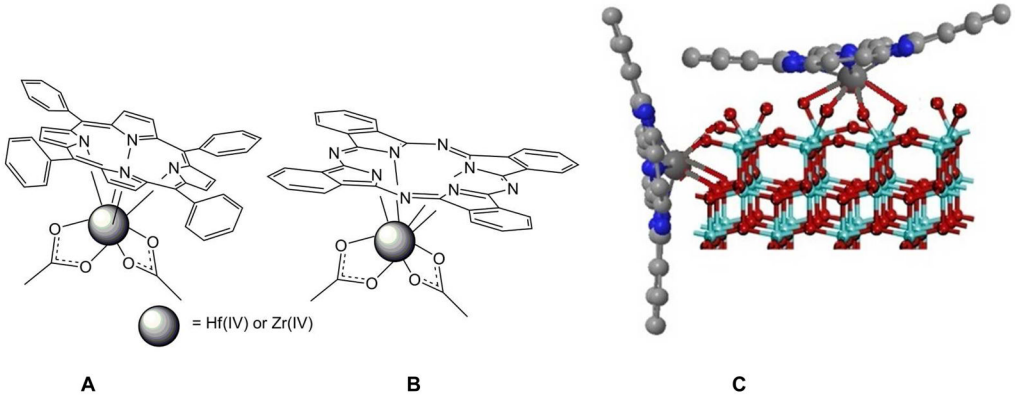

Figure 2.
(A) The porphyrinato compounds (TPP)Hf(OAc)$_2$ and (TPP)Zr(OAc)$_2$ used. (B) The phthalocyaninato compounds (Pc)Hf(OAc)$_2$ and (Pc)Zr(OAc)$_2$ used. Heating a slurry of TiO_2 nanoparticles with any of the dyes exchanges the acetates for the oxides on the nanoparticle surface, where (C) illustrates a proposed mode of binding of the metalloPc complexes to anatase TiO_2 (dark grey=metal ion, grey=carbon, blue=nitrogen, aqua=titanium, red=oxygen); anatase TiO_2 structure taken from Selloni, ref. 61.

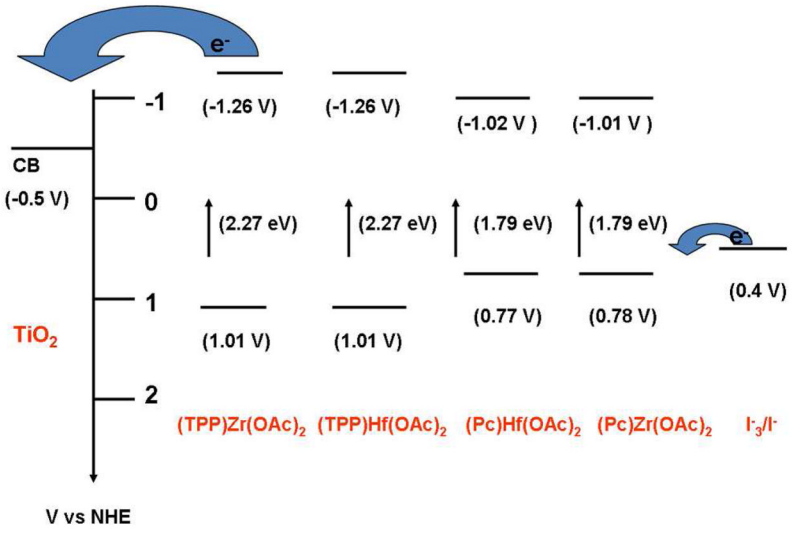

Figure 3.
Energy level diagram of the device components: the four metallodyes, TiO_2, and the I_3^-/I^- pair. Values in V referenced versus NHE.

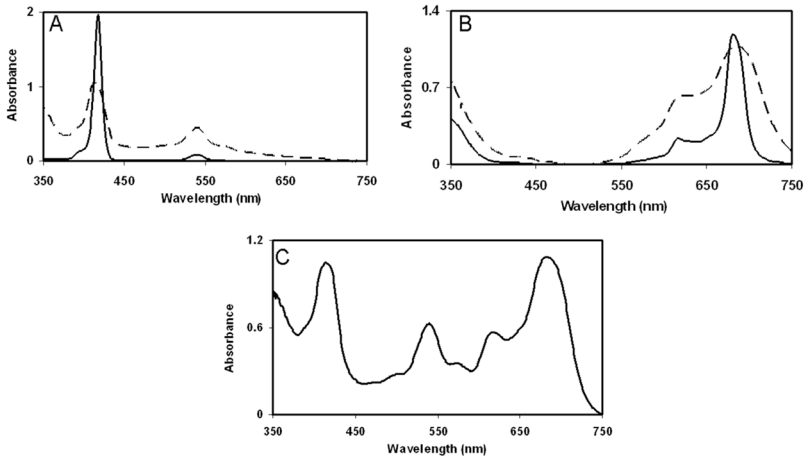

Figure 4.

(A) UV-visible spectra of (TPP)Zr(OAc)$_2$. in toluene (solid line), reflectance spectrum of a ~1 mm film of TiO_2 nanoparticles coated with (TPP)Zr(dashed line); **(B)** UV-visible spectra of (Pc)Zr(OAc)$_2$. in toluene (solid line), reflectance spectrum of a ~1 mm film of TiO_2 nanoparticles coated with (Pc)Zr(dashed line). **(C)** Reflectance spectrum of a ~1 mm film of TiO nanoparticles coated with both (TPP)Zr and (Pc)Zr. The dynamic range of the reflectance integrating sphere is ~1 absorbance units.

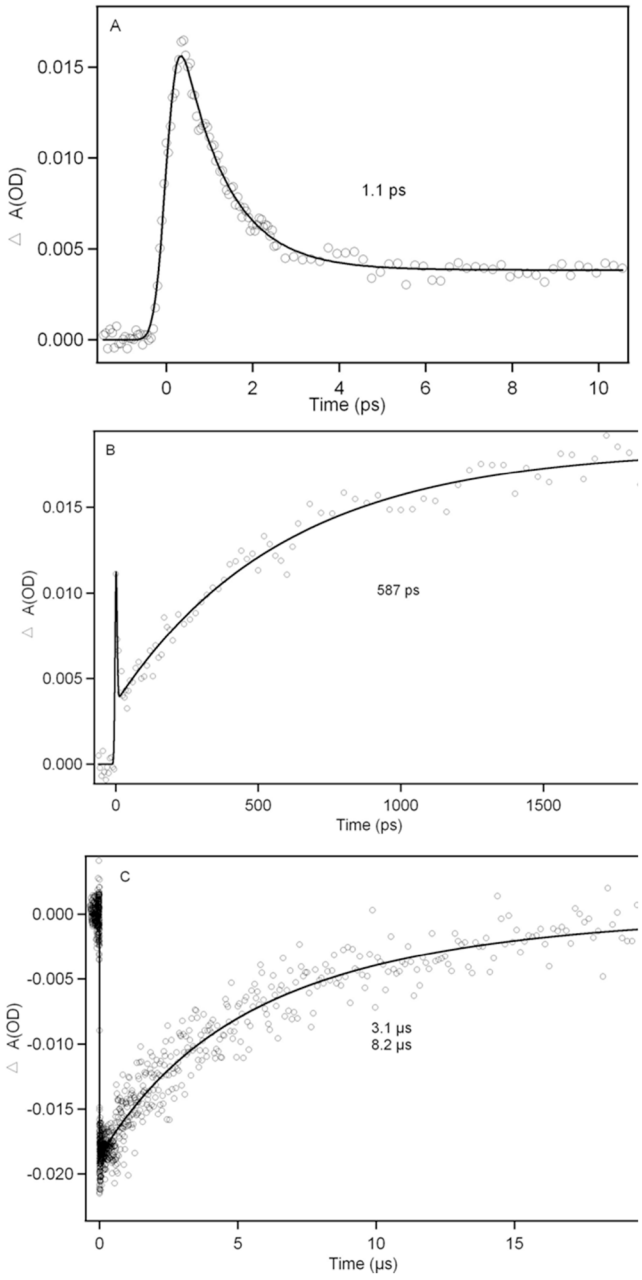

Figure 5.

Femtosecond transient absorbance of $(TPP)Zr(OAc)_2$. λ_{pump} = 420 nm, λ_{probe} = 633 nm. Solid lines are fits of the experimental data for electronic relaxation within S_1, (A) τ=1.1 ps; (B) τ= 587 ps; (C) Deactivation kinetics of $(TPP)Zr(OAc)_2$ in argon saturated toluene pumped 420 nm, when probed at 540 nm, the fit of the curve is bi-exponential with two lifetimes τ_1 ~3.1 μs and τ_2 ~8.2 μs. The transient absorbance of $(TPP)Hf(OAc)_2$ is similar (Figure S14).

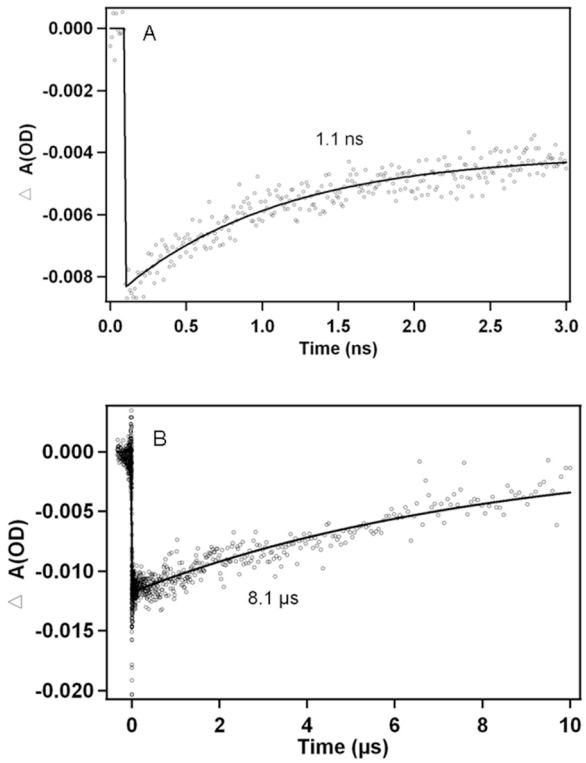

Figure 6.

Transient absorbance of (Pc)Zr(OAc)$_2$; λ_{pump}= 685 nm, λ_{probe} = 695 nm. Solid lines are fits of the experimental data of the singlet excited state decays. (A) τ ~ 1 ns; (B) in deaerated toluene τ ~ 8.1 μs.

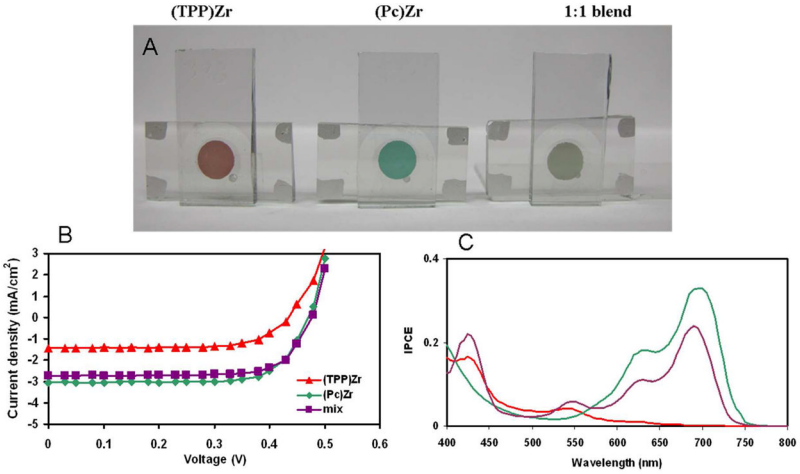

Figure 7.

(A) (TPP)Zr, (Pc)Zr, and a 1:1 mixture of (TPP)Zr: (Pc)Zron TiO_2 in DSSC; (B) Photocurrent-voltage characteristics of the solar devices after 1 h of light soaking and 5 days, sensitized with (TPP)Zr (red), (Pc)Zr (green), and a 1:1 mixture of (TPP)Zr and (Pc)Zr (purple); (C) Incident-photon-to-current efficiency action spectra for the same devices, same color scheme.

Table 1

Excitation Energy, Ground State and Excited State Oxidation Potentials of the Dyes.

Vs. NHE	[a] $E_{1/2}(S/S^+)$(V)	[b] $E_{0\text{-}0}$ (eV)	[c] $E_{ox}^*(S^*/S^+)$(V)
$(TPP)Zr(OAc)_2$	1.017	2.27 (545 nm)	−1.26
$(TPP)Hf(OAc)_2$	1.012	2.27 (545 nm)	−1.26
$(Pc)Hf(OAc)_2$	0.769	1.79 (690 nm)	−1.02
$(Pc)Zr(OAc)_2$	0.780	1.79 (690 nm)	−1.01

[a] $E_{1/2}(S/S^+)$ is the ground state oxidation potential;

[b] $E_{0\text{-}0}$ is the excitation energy;

[c] $E_{ox}^*(S^*/S^+)$ is the oxidation potential of the excited state; $E_{ox}^*(S^*/S^+)=E_{1/2}(S/S^+) - E_{0\text{-}0}/F$.

Table 2

Ground and Excited State Characteristics of Dyes in Toluene Solution at Room Temperature

Complexes	λ_B^{max}, nm	λ_Q^{max}, nm		λ_F^{max}, nm		λ_{Ph}^{max}, nm	Stokes Shift	Φ_F	τ_F, ns
	$S_0 \rightarrow S_2$	$S_0 \rightarrow S_1$		λ_{ex}	$S_1 \rightarrow S_0$	$T_1 \rightarrow S_o$			
(TPP)Hf(OAc)$_2$	418	539		418	550 580 633	715	10	0.003	0.05
(TPP)Zr(OAc)$_2$	416	539		416	550 580 633	--	10	0.02	0.6
(Pc)Hf(OAc)$_2$	334	614	684	615	695 730	--	10	0.01	<0.2
(Pc)Zr(OAc)$_2$	336	615	685	615	694 730	--	10	0.03	2
(TPP)Zn[a]	423	550	595		600 650	770	5	0.03	2
(Pc)Zn[b]	338	618	675		685 750	1100	10	0.20	2–3

[a] in toluene ref. 64,

[b] in DMSO ref. 70

Table 3

Lifetimes from Transient Absorbance of Dyes in Toluene

Complex	λ_{probe} (nm)	τ_1, ps $S_2 \rightarrow S_1$	τ_2, ps $S_1 \rightarrow S_0$	τ_3, ns in air $T_1 \rightarrow S_0$	τ_3, μs in Ar $T_1 \rightarrow S_0$
$(TPP)Hf(OAc)_2$	540	1.5	55	672	4.8; 25
$(TPP)Zr(OAc)_2$	540	1.1	587	--	3.1; 8.2
$(Pc)Hf(OAc)_2$	695	--[a]	138	225	2.0
$(Pc)Zr(OAc)_2$	695	--[a]	1020	223	8.1

[a] outside the range of the instrumentation. Upconversion experiments yield similar results. For comparison, the lifetimes for TPP = 12 ns, (TPP)Zn = 2 ns, (Pc)Zn = 2–3 ns.

Table 4

Photovoltaic Performance of DSSC Sensitized with 0.1 mM (TPP)Zr and (Pc)Zr Dyes Under Full 1.5 AM Illumination. The Active Area of the Device is 0.0707 cm^2.

Dye	Light soaking time	V_{oc} (V)	J_{sc} (mA/cm^2)	FF	η (%)
(TPP)Zr	after assembly	0.45	0.73	0.77	0.26
	after 5 days, 1 h light soaking	0.43	1.43	0.70	0.43
	after 9 days, total of 3 h light soaking	0.48	1.59	0.63	0.47
(Pc)Zr	after assembly	0.51	1.51	0.75	0.57
	after 5 days, 1 h light soaking	0.47	3.10	0.73	1.05
	after 9 days, total of 3 h light soaking	0.47	3.05	0.68	0.97
(TPP)Zr + (Pc)Zr	after assembly	0.53	1.34	0.75	0.54
	after 5 days, total of 1 h light soaking	0.48	2.74	0.74	0.97
	after 9 days, total of 3 h light soaking	0.50	2.70	0.74	0.99

J Phys Chem C Nanomater Interfaces. Author manuscript; available in PMC 2013 August 02.